Available online at www.sciencedirect.com
SCIENCE DIRECT
Journal of Catalysis 233 (2005) 359–371
JOURNAL OF CATALYSIS
www.elsevier.com/locate/jcat

Vanadium-containing ordered mesoporous silicates: Does the silica source really affect the catalytic activity, structural stability, and nature of vanadium sites in V-MCM-41?

S. Shylesh, A.P. Singh *

Catalysis Division, National Chemical Laboratory, Pune 411 008, India

Received 28 February 2005; revised 3 May 2005; accepted 3 May 2005

Available online 13 June 2005

Abstract

A series of vanadium-substituted mesoporous materials were synthesized hydrothermally with the use of two commonly used silica sources, fumed silica and tetra ethyl orthosilicate. The extent of mesopore structural ordering was confirmed from X-ray diffraction, N_2 physisorption, SEM, and TEM, and the presence and nature of vanadium species inside the framework of the MCM-41 matrix was confirmed in detail with the use of various characterization techniques like FT-IR, ^{29}Si MAS NMR, DRUV–vis, EPR, ^{51}V MAS NMR, and Raman analysis. It is deduced from the above characterization techniques that, regardless of the silica source, vanadium is incorporated into the silica framework and thereby increases the structural ordering and wall thickness of the mesoporous material. Thermal and hydrothermal studies performed over the V-MCM-41 catalysts show that the Si–O–Si inorganic backbone from a fumed silica source is more resistant to severe thermal treatments and hydrolysis than the tetraethyl orthosilicate-synthesized catalysts. Spectroscopic characterization reveals the existence of easily accessible isolated tetrahedral vanadium sites on V-MCM-41 catalyst prepared from fumed silica catalyst, whereas the sample obtained from a tetraethyl orthosilicate silica source shows vanadium in more disordered sites. Catalytic results show that both catalysts display excellent activity toward the epoxidation reaction of bulkier olefins, and the exceptional activity of the fumed silica catalyst may arise from the more isolated tetrahedral sites and the complementary textural characteristics, which may facilitate the easy access of substrate to the isolated framework metal sites.

Keywords: Vanadium; MCM-41; Fumed silica; Tetraethyl orthosilicate; Epoxidation

1. Introduction

MCM-41, a typical member of the M41S family of mesoporous molecular silicates, had attracted considerable attention as a catalyst support for the processing of bulkier molecules, because of its large surface area (∼1000 m^2/g), uniform pore size (15–100 Å), and high-density surface silanol sites [1]. Numerous studies had been devoted after its discovery to surface modification in order to increase its structural stability and thereby to utilize its unique property in various fields such as separation science, host-guest chemistry, optoelectronics, etc. [2–4]. Even though it is an attractive candidate, pure siliceous MCM-41 shows limited applications in various organic transformations, and hence modification of this material by the introduction of various active metal sites is necessary for its utility in catalysis. Thus the isomorphous replacement of silicon with transition metals or postsynthesis metal modification (impregnation/grafting) helps to create well-defined heterogeneous catalysts for designed applications [4,5]. However, there is considerable debate over the stability of metal-containing mesoporous materials prepared by various routes, and in a more generalized way it is argued that the isomorphously substituted metal species on the silicate framework would not leach easily un-

* Corresponding author. Fax. +91 2025893761.
E-mail address: apsingh@cata.ncl.res.in (A.P. Singh).

0021-9517/$ – see front matter
doi:10.1016/j.jcat.2005.05.001

der reaction conditions and hence exist as true heterogeneous catalysts!

Apart from Ti-MCM-41, one of the well-studied metal-containing mesoporous materials is V-MCM-41, because of its catalytic potential for selective oxidation reactions with aqueous H_2O_2/TBHP as oxidants [6–9]. Even though Reddy et al. [6] had first successfully synthesized vanadium-substituted MCM-41, a detailed characterization of these materials was carried out independently by Tuel et al. [10] and Luan et al. [11], and they concluded from their studies that (i) vanadium centers in the as-synthesized and calcined forms of V-MCM-41 had the same coordination state, and no direct chemical bonding was formed with the silicate frame work, and (ii) vanadium occurs simultaneously in two forms on the support surfaces, as framework and extraframework species. Even after a decade, there is still much research in this area, and arguments continue over the assignment of various bands for these mesoporous materials; hence concluding evidence is still needed to identify the exact species formed. Apart from these discrepancies, the stability/heterogeneity of vanadium-containing materials under severe reaction reactions is highly limited, and hence careful and detailed investigations are needed to account for the observed catalytic activity behavior [12,13]. Usually hydrothermal and thereby structural stability are the two important factors that determine the applicability of any mesoporous material in liquid-phase oxidation reactions. Actually the solid wall surfaces between the mesopores are too delicate to withstand severe reaction conditions, and hence a rapid disorder in mesoporosity is observed after drastic reaction conditions, which may enhance the leaching of framework substituted metal species to the reaction mixture and thereby limit its further usability. Hence it is of paramount importance to devote more attention to modification of the surface of the mesoporous materials for its wide applicability and reusability.

It is known that increased hydrothermal stability of mesoporous materials is related to an increase in the degree of silicate condensation, and hence control of the pH of the gel mixtures had been efficiently utilized in the synthesis of high-quality mesoporous materials [14]. Alternatively, prolonged stirring time plus hydrothermal treatments at higher temperatures ($>150\,^{\circ}C$) are also employed to increase the stability of the mesoporous materials. However, the latter method suffers from numerous drawbacks, like the dissolution/decomposition of the micelles and further possible phase transformations due to the increased tail motion of the surfactants. Hence it is reasonable that the cooking parameters had a prominent effect on the structural perfection, percentage of metal incorporation, and stability. Even though vanadosilicates are the subject of a greater percentage of the literature reports on M-MCM-41 materials, thorough and systematic investigations of the stability and nature of vanadium sites are scarce, and hence the present study was undertaken to probe in detail the effect of silica sources in the synthesis of V-MCM-41 materials. Since it is known that the activity and selectivity of vanadium-containing materials are very sensitive to the nature and coordination of vanadium ions, it is crucial to verify whether the silica source had a role in the nature of vanadium sites and in their further structural stability [7].

In the present work, we investigated in detail the nature of vanadium species formed on different silica sources (fumed silica and tetraethyl orthosilicate), in order to (i) uncover the structural property/stability difference in Si-MCM-41 and V-MCM-41 materials under different silica precursors and, (ii) determine whether the silica source had a role in the incorporation and nature of vanadium species in V-MCM-41 materials. The stability and heterogenity of the developed materials were further verified in the epoxidation reaction of cyclooctene, through a series of heterogenity studies.

2. Experimental

Vanadium-incorporated molecular sieves and pure siliceous MCM-41 were synthesized hydrothermally in the temperature range of $100\,^{\circ}C$, with vanadyl sulfate ($VOSO_4 \cdot 3H_2O$; Aldrich) as the vanadium source and fumed silica (SiO_2, 99.8%; Aldrich) and tetraethyl orthosilicate (TEOS, 98%; Aldrich) as the silica source.

2.1. Synthesis procedure

Vanadium-incorporated mesoporous materials were synthesized by a one-pot synthesis procedure with the use of a gel composition of

$$SiO_2{:}x\ VO_2{:}0.17\ Na_2O{:}0.5\ HDTMABr{:}100\ H_2O,$$

where HDTMABr is hexadecyl trimethyl ammonium bromide and x varies from 0.025 to 0.012. Typically, an aqueous solution of HDTMABr and vanadyl sulfate was added slowly to a vigorously stirred solution mixture of fumed silica/TEOS in alkaline condition. The mixture was stirred at room temperature for 5 h and then subsequently autoclaved at $100\,^{\circ}C$ for 4 days. For comparison purposes, respective silica polymorphs are also prepared by the same method, but without the addition of vanadyl sulfate. The solid material obtained was then filtered and washed well with copious amounts of water, until the filtrate showed a neutral pH, and then dried at $80\,^{\circ}C$ for 3 h. The surfactant occluded inside the pores of the mesoporous material was removed by calcination at $540\,^{\circ}C$ for 6 h, at a heating ramp of $1\,^{\circ}C/min$, as the mesostructure of the materials is seriously affected at higher heating temperature rates. To evaluate the hydrophobicity of the material, both VMS and VMT samples ($Si/V = 55$) were silylated under a nitrogen atmosphere with dimethyl dichloro silane (Aldrich) as the silylating agent. For that, 1 g of dimethyl dichloro silane in dry toluene was added dropwise to a stirred solution mixture of calcined V-MCM-41 sample (1 g) in 50 ml toluene. The solution was then allowed to reflux for 6 h, and finally the materials were filtered,

washed with toluene, and then soxhlet extracted with a mixture of diethyl ether (100 ml) and dichloro methane (100 ml) for 12 h. The materials were then dried at 80 °C for 3 h. The solid materials obtained from fumed silica sources are denoted by VMS, the materials from TEOS are denoted by VMT, and the corresponding silica sources are referred to as SMS and SMT.

2.2. Characterization

Powder X-ray diffraction patterns of as-synthesized and calcined samples were recorded on a Rigaku D MAX III VC (Ni-filtered Cu-K_α radiation, $\lambda = 1.5404$ Å between 1.5° and 10° (2θ), with a scanning rate of 1°/min). The specific surface area, total pore volume, and average pore diameter were measured by the N_2 adsorption–desorption method with a NOVA 1200 (Quanta chrome) instrument. Samples were activated at 200 °C for 3 h under vacuum, and then the adsorption–desorption was conducted by passing nitrogen into the sample, which was kept under liquid nitrogen. Pore size distribution (PSD) was obtained from the adsorption branch of the isotherms by the Barret–Joyner–Halenda (BJH) method. TG-DTG and DTA measurements were carried out on a Mettler Toledo 851 instrument with an alumina pan under an air atmosphere (80 ml/min) from ambient to 1000 °C at a heating rate of 10 °C/min. SEM micrographs of the vanadium-containing samples were obtained on a Leica Stereoscan 440 instrument, and the TEM images were obtained on a JEOL JEM-1200 EX instrument with 100-kV acceleration voltages to probe the mesoporosity of the material.

FTIR spectra of the solid samples were taken in the range of 4000 to 400 cm^{-1} on a Shimadzu FTIR 8201 instrument. Diffuse-reflectance UV–vis spectra of powdered samples were recorded with a Shimadzu UV-2101 PC spectrometer equipped with a diffuse-reflectance attachment, with $BaSO_4$ as the reference. For monitoring of the spectra of hydrated samples, the catalyst were kept under ambient conditions for 2 h, whereas for dehydrated samples the catalyst were treated in a dry air atmosphere at 550 °C for 5 h and flushed with an inert atmosphere, repeatedly, before the spectra were recorded. The absorption edge energy values were determined from the energy intercept of a linear fit passing through the near-edge region in a plot of $[F(R_\alpha)h\nu]^{1/2}$ versus $h\nu$, where the first parameter refers to the Kubelka–Munk (KM) function and $h\nu$ is the energy of incident photons. EPR spectra of the solid samples were recorded at room temperature (25 °C) at X-band frequency on a Bruker EMX spectrometer. The solid-state ^{29}Si MAS NMR spectra were recorded on a Bruker MSL 300 NMR spectrometer with a resonance frequency of 59.6 MHz. Finely powdered samples were placed in 7.0-mm zirconia rotors and spun at 2.5–3.5 kHz, with TMS as the reference compound, and ^{51}V MAS NMR was recorded under a magnetic field of 7.05 T, spinning at 7 kHz, and was referenced to ammonium metavanadate. Raman measurements were performed with a Jobin Yron TRIAX 550 triple grating spectrometer equipped with a cryogenic charge-coupled device camera and a diode-pumped, frequency-doubled, solid-state Nd:YAG laser of 532 nm (model DPSS 532-400; Coherent Inc, USA).

2.3. Catalytic tests

Epoxidation reactions were performed in a round-bottomed glass batch reactor fitted with a water-cooled condenser, with aqueous H_2O_2 (30%) and TBHP (70%) as oxidants. Reactant mixtures of cyclooctene (0.92 g, 8.3 mmol), H_2O_2 (0.26 g, 2.2 mmol), and acetonitrile solvent (5 g, dried over 4 Å molecular sieves) were added to catalysts (10% of substrate) and heated with an oil bath at a temperature of 70 °C with magnetic stirring (ca. 800 rpm). After reactions, the reaction mixture was cooled to room conditions, the catalyst was separated from the reaction mixture by centrifugation, and the oxidized products were analyzed on a gas chromatograph (HP 6890) equipped with a flame ionization detector (FID) and a capillary column (5 μm cross-linked methyl silicone gum, 0.2 mm × 50 m) and were further verified by GC-MS (Shimadzu 2000 A). The presence of unreacted oxidant at the end of each reaction was checked by means of standard iodometric titrations.

3. Results and discussion

3.1. Physical properties

XRD patterns of V-MCM-41 samples prepared from the two silica sources given in Fig. 1 show some important differences in the long-range ordering and in the intensity of the characteristic diffraction peaks. Even though it is known that a higher hydrothermal synthesis temperature can be used to incorporate a greater percentage of metal into the silica framework, the sequential problem of the dissolution of the micelles at higher temperatures, which may largely

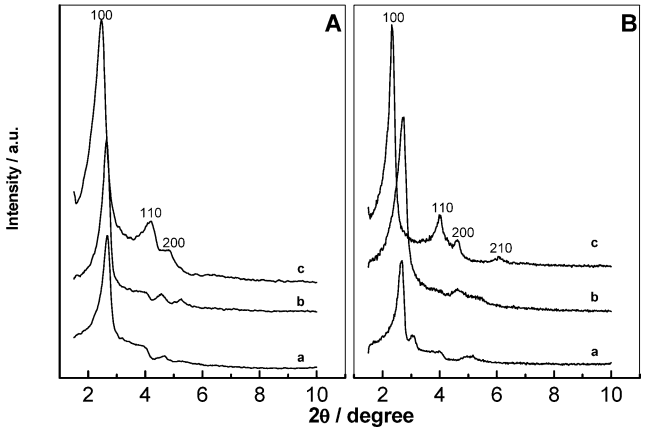

Fig. 1. XRD patterns of (A) VMT catalysts and (B) VMS catalysts, where (a) Si/V (80), (b) Si/V (55) and (c) Si/V (25).

Table 1
Textural characteristics of vanadium-containing mesoporous materials

Catalyst	V[a] (wt%)	Unit cell shrinkage (%)	S_{BET} (m^2/g)	V_p[b] (cc/g)	D_p[c] (Å)	Wall thickness[d] ω_t (Å)	$Q^4/(Q^3+Q^2)$[e]
VMS (25)[f]	0.98	4.07	852	0.61	25.10	16.38	
VMS (55)	0.67	10.07	909	0.53	23.83	15.72	2.04
VMS (83)	0.36	12.43	828	0.48	22.97	15.63	
SMS	0.0	14.80	711	0.37	21.99	14.52	1.63
VMT (25)	0.76	0.87	1103	1.0	25.22	18.38	
VMT (55)	0.50	9.51	1060	0.81	21.64	17.15	1.15
VMT (83)	0.21	10.13	1036	0.63	20.96	16.55	
SMT	0.0	10.31	905	0.56	19.39	16.05	0.84

[a] Vanadium content determined by ICP-OES analysis.
[b] V_p = pore volume.
[c] D_p = pore diameter.
[d] Wall thickness $= a_0 - D_p$, where $a_0 = 2d_{100}/\sqrt{3}$.
[e] Relative peak area from ^{29}Si MAS NMR.
[f] Numerals in parentheses stands for the Si/V gel ratios.

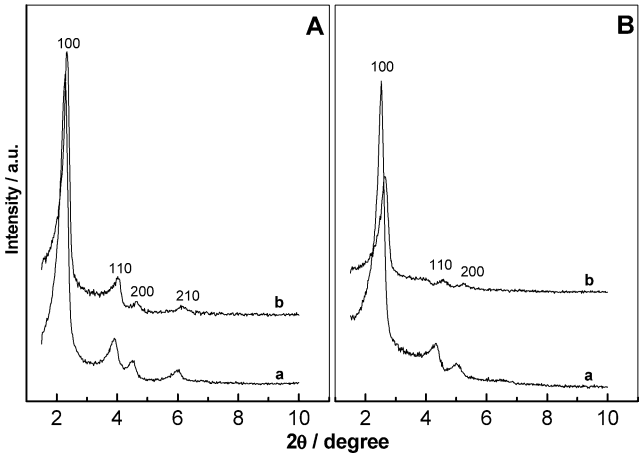

Fig. 2. XRD patterns of (A) VMT catalysts and (B) VMS catalysts; where (a) stands for as synthesized and (b) stands for calcined catalysts.

affect the long-range structural ordering, limits the present hydrothermal treatments at 100 °C, but with more cooking time. Recently we reported the synthesis of V-MCM-41 material prepared under the mentioned gel ratio (see Section 2), but with an H_2O/Si ratio of 60, where we observed that when the Si/V ratio is 30, XRD patterns show broad reflections, with a corresponding decrease in intensity of the long-range-ordered peaks [15]. Hence, in the present case, we had changed the H_2O/Si ratio to 100, and, interestingly, high-quality XRD patterns are observed for V-MCM-41 materials with a Si/V ratio of even 25. These results suggest the importance of homogeneous gel mixtures in the synthesis of Si-MCM-41- and M-MCM-41-related materials, where the presence of excess water may make it easier to orient the surfactant–silicate assembly than it would be under thick gel conditions. Furthermore, it is reasonable to assume that the addition of more water may increase the effective head group area of the surfactants, which in turn may reduce the packing parameter value ($g = V/a_0 l$), resulting in materials of good quality [16]. Indeed, Lim et al. [17] also observed a similar observation of the effect of water and noticed that excess water helps to incorporate a higher percentage of vanadium ions into the silicate framework. However, the reproducibility of that procedure is not promising, whereas the present synthesis protocol is reproducible, but a slight decrease in the percentage of metal incorporation is noted with water content, which may be due to the difference in other gel ratios. A comparison of the XRD patterns of the respective siliceous counterparts and vanadium-containing mesoporous materials shows a linear increase in the lattice parameter values and a better structural perfection with increasing percentage of vanadia loading; the results obtained are listed in Table 1. These discrepancies apparently show the effect of vanadium in the synthesis gel, as its salt-like influence may help to orient the surfactant–silicate assembly in a more ordered way than under metal-free systems. Thus even though the same surfactant was used for the synthesis of vanadium-containing mesoporous materials and its corresponding silica counterparts, the large discrepancies may arise for the following reasons: (i) due to the larger V–O bond distance than the Si–O bond distance, and (ii) the thickening of the pore wall due to transition-metal-promoted cross-linking of the amorphous silica walls. In order to ascertain this, TG-DTA analysis of V-MCM-41 materials and their corresponding silica analogues was performed (figure not shown). The typical weight loss curves obtained show that the entire template, including water adsorbed on the pore channels, is decomposed at a temperature of 400 °C, and a total weight loss of ∼45% is observed for both the VMS and VMT catalysts. However, a comparative analysis of the V-MCM-41 samples with the corresponding analogous silica shows that the percentage weight loss is larger in V-MCM-41 catalysts than Si-MCM-41 materials (35–40%). These results support the assumption of the increased structural ordering of the M-MCM-41 samples due to increased surfactant–silicate assembly in the presence of metal salts compared with metal-free conditions.

Fig. 2 further presents the XRD patterns of VMS and VMT catalysts in their as-synthesized and calcined forms. The well-defined diffraction patterns of as-synthesized V-MCM-41 samples can be indexed to the Bragg reflections 100, 110, 200, and 210, characteristic of materials with long-range hexagonal ordering, and their intensities are well pronounced. However, after calcination, although both materials retain their long-range-ordered features, the fumed silica synthesized vanadium catalyst shows XRD patterns with an approximately twofold lower intensity than those of the TEOS synthesized catalyst. This surprising result may relate to the difference in the nature of silanol condensation and thus indicates that the silica source had a role in the quality of MCM-41 materials. Thus, in order to ascertain these discrepancies, one has to probe in detail the chemistry behind the nature of hydrolysis and its further condensation procedures when using silica sources of a different nature. Tetra ethyl orthosilicate, a quarternary alkoxide with

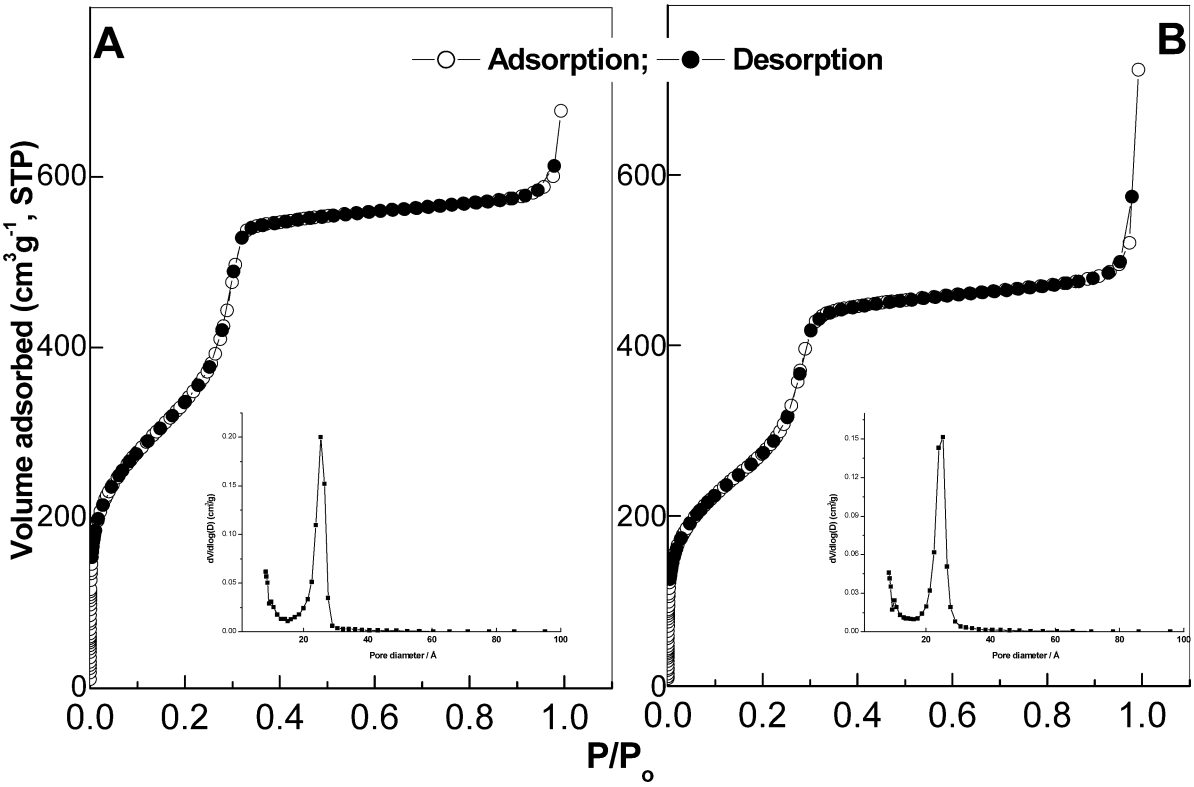

Fig. 3. Nitrogen adsorption–desorption isotherms and pore size distribution profiles (inset) of (A) VMT (Si/V = 25) and (B) VMS (Si/V = 25) catalysts.

a monomeric structure, produces silicate species of smaller chains during its hydrolysis and subsequent condensation steps. In contrast, the fumed silica source, itself polymeric in nature, produces oligomeric silicates of larger sizes, and hence the condensation of such silica species around the micelles is faster, producing materials of good quality [14]. However, during calcination the remaining silanol groups may be condensed faster, thereby increasing the wall thickness of the materials at the expense of (100) face intensity. But the increased intensity of the TEOS-prepared materials after calcination may be due to the following factors: (i) During hydrolysis, the precursor TEOS produced ethanol as a by-product, and we feel that the formed alcohol had a significant role in the formation of well-ordered, XRD patterns that were more intense than those produced by the VMS catalysts, by increasing the curvature between the surfactant-silicate species. Since the formed ethanol can accumulate near the hydrophilic surfactant head group, the effective area of the surfactant is increased, and these in turn may reduce the packing parameter values, resulting in hexagonal mesoporous materials of high quality. (ii) Due to the decreased silicate condensation. These results are further supported by the increased lattice contraction exhibited by the VMS materials compared with the VMT materials and are usually related to the extent of cross-linking of the noncondensed residual silanol groups upon calcination (Table 1). Thus the significant lattice contraction observed for the VMS catalyst obviously shows the more fully cross-linked inorganic framework, when a silica source of a polymeric nature is used as the inorganic backbone. These results had great significance, especially in the liquid-phase oxidation reaction of M-MCM-41 materials with aqueous H_2O_2 as oxidant, as the water present in the oxidant can cause the thin frame walls of mesoporous silicates to seriously deteriorate and enhances the leaching of the isomorphously substituted metal sites. Thus the nature of the silica precursor used in the synthesis of Si(V)-MCM-41 materials plays a key role in affecting the overall structural stability of MCM-41 materials, which in turn may arise from the rate of hydrolysis and subsequent condensation procedures. Moreover, the absence of peaks corresponding to crystalline V_2O_5 in any of the preparation methods shows that the metal ions were either atomically dispersed in the framework positions or may exist in an amorphous dispersed form on the outside framework of mesoporous supports.

To further confirm the mesopore structural ordering, N_2 physisorption analysis was also performed, since if the material had a regular pore structure it would show a steep increase in adsorption isotherms, because of the capillary condensation at specific N_2 partial pressures. N_2 adsorption–desorption isotherms of all samples show an inflection in the P/P_0 range of 0.2–0.4, with completely reversible isotherms, but without any hysteresis loops, characteristic for ordered mesoporous materials of Type IV; the physisorption results for the samples prepared with different silica sources and their corresponding pore size distribution curves are depicted in Fig. 3. Since a surfactant with the same chain length (C_{16}-) was used for the synthesis of Si-MCM-41

materials and vanadium-containing mesoporous materials, an almost similar pore size is expected in all cases. However, the observed increase in pore size after vanadium substitution shows the effect of metal salts in the synthesis procedures and in the subsequent hydrothermal treatments (Table 1). Usually metal (here, vanadium) is incorporated into the silica framework of mesoporous materials in two ways: (i) Part of the vanadium may be distributed along the pore walls and may combine with the hydroxyl groups to form a tetrahedral environment, while another part may be well exposed on the pore wall surfaces as external surface species, causing a possible decrease in the pore size and pore volume. (ii) Vanadium is incorporated deep into the silica framework with tetrahedral coordination causing a possible increase in the pore size [17]. For zeolites, metal incorporation usually increases its pore size because of the crystalline framework and the longer bond length of M–O groups than Si–O groups. However, such a clarification is not possible in MCM-related materials because of its amorphous structure, in which an increase or a decrease in pore size is usually observed with the experimental protocols. Thus the former way of incorporation does not cause any significant change in the pore size values, whereas the latter way of incorporation may increase the channel width and hence exhibits larger pore sizes than the corresponding silica support surface. In the present study, it is observed that regardless of the silica source, the pore size and surface area of the samples increase with increasing percentage of vanadia loading. For instance, the support SMS shows a surface area of 711 m^2/g, and an increase of 141 m^2/g is observed for the VMS (25) catalyst, whereas the VMT (25) catalyst shows an increase of ∼22% from its corresponding silica polymorph. The increase in pore size of vanadium-containing materials compared with the respective silica polymorphs shows that vanadium gets incorporated inside the silica framework; if this occurs deep within the silica framework, an increase in pore width is expected, because of the larger V–O bond distance (1.8 Å) compared with the Si–O bond distance (1.6 Å) [17]. For better insight, we also examined the thermal and hydrothermal stabilities of the VMS and VMT materials by increasing the calcination temperature to a high value of 800 °C and by conducting water treatments for as long as 24 h; the changes observed in the surface area are depicted in Fig. 4. It is interesting to note that the VMT catalyst shows a complete loss of surface area after 800 °C calcinations, and a decrease of 70% is observed after 24 h of water vapor exposure, whereas the VMS catalyst shows only a moderate decrease of 50 and 17%, respectively, after drastic thermal and hydrothermal treatments. These results further support the findings from the XRD measurements and show the increased thermal and hydrothermal stability of the V-MCM-41 catalyst prepared from the fumed silica source. Thus the increased thermal resistance and hydrothermal stability of the VMS catalyst arise reasonably from the increased silicate condensation, as explained, thereby confirming that the silica source had a significant role in the physical properties of the synthesized V-MCM-41 catalysts.

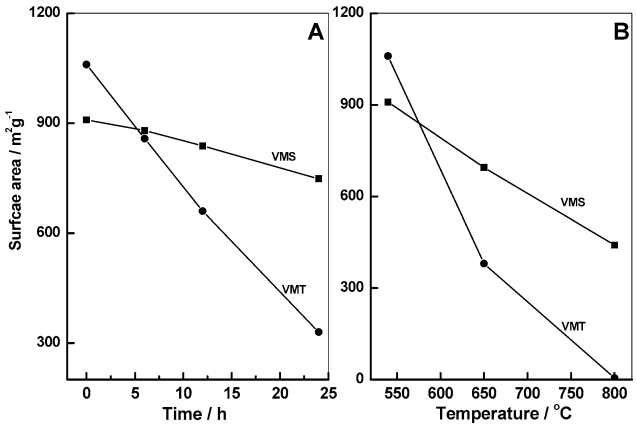

Fig. 4. Surface area differences as a function of (A) water vapor exposure rate and (B) calcination temperature on V-MCM-41 catalysts.

The particle size and morphology of the VMS and VMT catalysts determined from the SEM analysis show that the use of different silica sources plays a role on the final morphology of the developed mesoporous materials (Figs. 5a and 5b). For instance, the VMT (55) catalyst shows a globular morphology with particles ∼0.2–0.5 μm in diameter, whereas the VMS catalyst shows flower-like structures ∼3–5 μm in diameter, thus showing that different silica sources can modify the morphological structure of MCM-41 considerably. Furthermore, the globular particles of V-MCM-41 materials synthesized from a TEOS silica source are smaller and less homogeneous (agglomerates) than the fumed silica catalyst, which is consistent with earlier reports [18]. However, TEM analysis performed on the present VMS and VMT catalysts shows a hexagonally arranged structure when they are viewed along the pore direction, further proving that the present materials are of high quality (Figs. 5c and 5d).

3.2. Spectroscopic characterization

FT-IR spectra of Si-MCM-41 and V-MCM-41 samples synthesized from different silica sources are depicted in Figs. 6A and 6B. The band observed at 800 cm^{-1} is due to the symmetric stretching vibrations of the Si–O groups, and the sharp band observed at 1080 cm^{-1} is assigned to the asymmetric stretching of the Si–O vibrations, and its increased intensity correlates with a higher concentration of the siloxane groups. Furthermore, a strong band is observed in the mid-infrared region at 960 cm^{-1} and is generally attributed to the incorporation of various heteroatoms at the framework positions of porous metallo-silicates. Since MCM-41 have properties between amorphous materials and zeolites, literature reveals with unambigituy for its assignment and are attributed to the presence of Si–O–V bands and/or to the perturbations in the rocking-mode vibrations of Si–OH moieties due to adjacent metal ions [19]. However, the shifting of 960 and 1090 cm^{-1} peaks to lower and higher

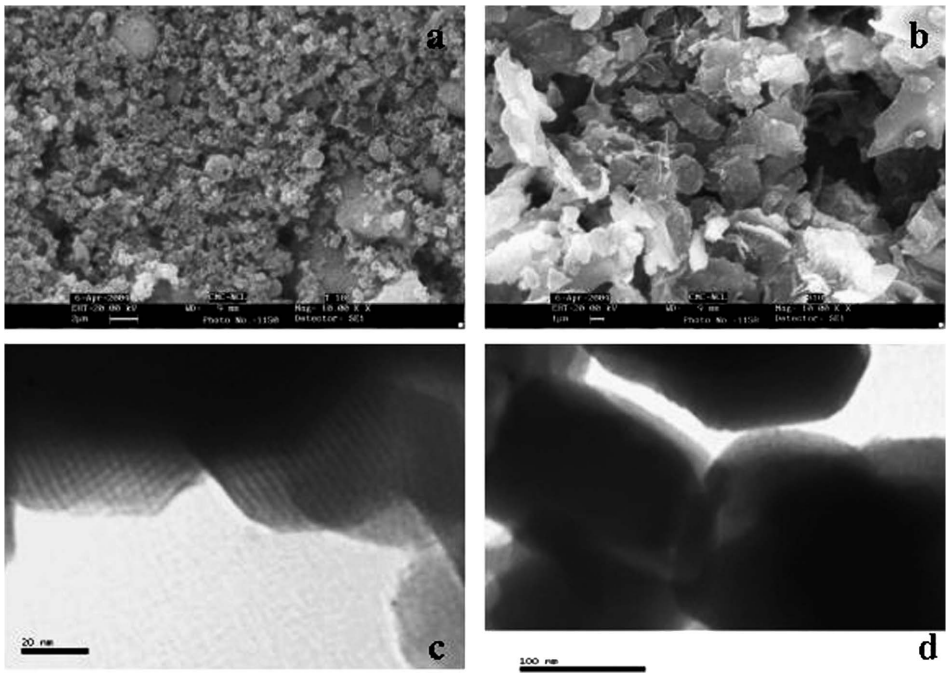

Fig. 5. Scanning electron micrographs of (a) VMT catalyst, (b) VMS catalysts and transmission electron micrographs of (c) VMT catalyst and (d) VMS catalyst.

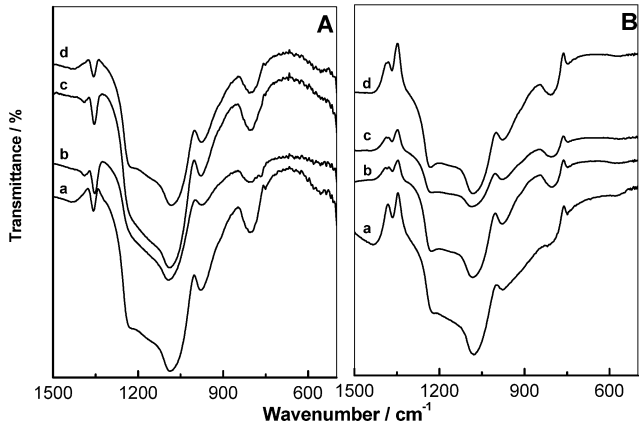

Fig. 6. FTIR spectra of (A) VMT catalysts and (B) VMS catalysts, where (a) $Si/V = \infty$, (b) $Si/V = 80$, (c) $Si/V = 55$ and (d) $Si/V = 25$.

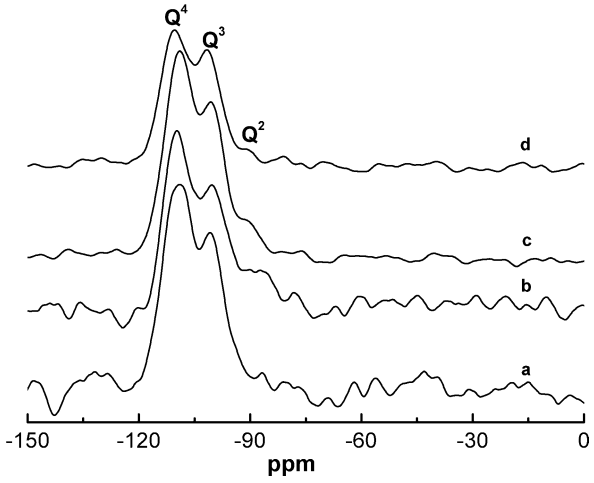

Fig. 7. ^{29}Si MAS NMR results of calcined Si-MCM-41 and V-MCM-41 materials; (a) SMS, (b) SMT, (c) VMS, (d) VMT.

frequencies, respectively, after metal substitution is usually taken as an indication of the presence of metal species in the framework of the mesoporous materials, and their increased intensities lead to better structural perfections. To further verify this band assignment, we had carried out silylation on the present VMS and VMT catalysts with dichloro dimethyl silane, with the assumption that the silylating agents may effectively consume the Si–OH groups, and thus the band observed in the 960 cm^{-1} range after silylation may reasonably arise from Si–O–V groups [15]. Moreover, the absence of peaks at 820 cm^{-1}, due to V–O–V deformation modes of crystalline V_2O_5, confirms the absence of agglomerated vanadia species in the present samples and is in accordance with the XRD results [20].

Fig. 7 shows the ^{29}Si MAS NMR results for calcined Si-MCM-41 and V-MCM-41 materials; their relative peak proportion values are given in Table 1. Because of the amorphous nature of silica walls and the presence of a wide range of T–O–T bond angles, M41S-related materials usually show broad peaks in the −90 to 110 region, and the bands are centered at −92, −100, and −110 ppm. These are assigned to the $Si(OSi)_x(OH)_{4-x}$ framework units, where x can have values of 2 (Q^2 site), 3 (Q^3 site), and 4 (Q^4 site). In the present synthesis, it is worth to noting the presence of Q^2 sites in the SMT catalyst, whereas similar sites are not observed in the spectra of Si-MCM-41 synthesized from a fumed silica source. Thus the decreased intensity (from

PXRD) of the fumed silica catalysts after calcination is related to more silanol condensation and thereby increases the wall thickness of the material at the expense of mesopore ordering. In addition, a significant decrease in the Q^3/Q^4 ratio with a peak broadening of the Q^4 site is observed for the V-MCM-41 samples compared with the silica counterparts. Thus the decrease in intensity of the Q^2 and Q^3 sites and the corresponding increase in the Q^4 site of V-MCM-41 materials may show that vanadium becomes substituted in the silica framework and promotes condensation of the uncondensed silanol sites [21]. These results once again support our assumptions mentioned in the XRD section, for an increased mesopore ordering and intensity of the V-MCM-41 samples compared with their silica counterparts, since the transition metals may act as a promoter for the condensation of the silicate species, thereby affecting the long-range ordering and wall thickness of the final mesoporous material.

Diffuse-reflectance UV–vis spectra are useful and reliable in the detection of the presence of framework and extraframework metal species in metal-containing mesoporous materials. For vanadium-containing mesoporous materials, direct information about the oxidation state and the possible dispersion of vanadia species can be derived from the color of the materials synthesized. The color of all V-MCM-41 catalysts is white after calcination (dehydrated), which turns yellowish (hydrated) during atmospheric exposures; the changes are more prominent for VMS catalysts, indicating a greater percentage of vanadia species on the wall surfaces. Thus the color transformation of the materials shows a possible modification in the oxidation state of the vanadia species from its original tetrahedral coordination to the square pyramidal/octahedral coordination by the coordination of two water molecules from the atmosphere, and the red shift increases with the percentage of vanadia loading. Furthermore, the significant color change in the V-MCM-41 materials during the rehydration process relates to the less crystallographic order in the pore walls and larger surface area and pore sizes of the MCM-41 matrix, where the water molecules can easily access the well-exposed isolated sites to change the coordination of the matrix from 4 to 6. Instrumentally, the UV–vis spectra of VMS and VMT catalysts show the presence of sharp bands at ∼260 and ∼340 nm for the tetrahedral V^{5+} ions inside the walls and the tetrahedral V^{5+} ions on the wall surfaces (extra framework species). However, for catalysts with a Si/V ratio greater than 55, the band after 300 nm is not prominent, even in the hydrated state, and this suggests that at lower vanadium contents nonaccessible tetrahedral vanadium sites may be the possible type of local environment present, where the water molecules cannot access the vanadia sites to increase the coordination. Moreover, as noted by Luan et al. [11], we also observed that the absorption in the 260-nm regions is not influenced by moisture treatments, whereas the bands above 300 nm are modified by various treatments (Fig. 8). This anomalous behavior is interpreted for the presence of two different kinds of vanadia species on the samples, one well

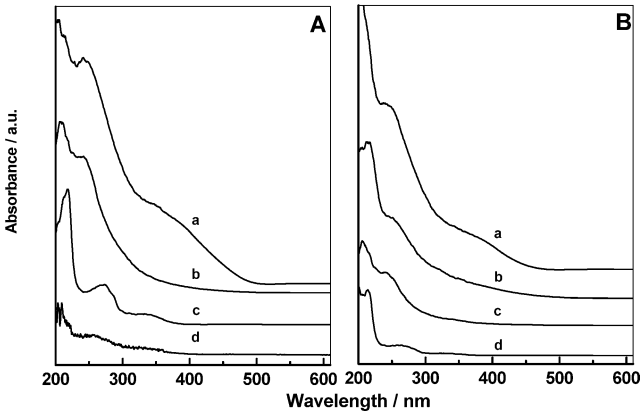

Fig. 8. DRUV–vis spectra of calcined V-MCM-41 materials recorded under ambient conditions (A) VMT catalysts and (B) VMS catalysts, where (a) Si/V (25), (b) Si/V (55) (dehydrated), (c) Si/V (55), (d) Si/V (80).

buried inside the pore channels, which are thermally and chemically stable, and the other on the hexagonal wall surfaces, which can easily undergo modifications. Hence in order to deduce the exact local environment of vanadium in the present samples and to further confirm the above results, we also made absorption edge energy measurements with a procedure reported by Barton et al. [22], using interpretations based on vanadium model compounds having known local symmetries. This principle, first applied by Weber [23] for a series of molybdenum-containing compounds, relates the band-gap energy and domain size, where the latter defines the nearest neighboring ligands and which are closely related to the local symmetry of metal ions. Hence the present series of catalysts is compared with vanadium model compounds of known symmetries. Thus the edge energy values calculated for V-MCM-41 materials lies in the 3–4-eV range, and hence it is reasonable to assume the formation of only tetrahedral V^{5+} species on both V-MCM-41 catalysts [24]. However, a comparison of the UV edge energy values of VMS and VMT catalysts shows that the catalyst prepared from fumed silica as the silica source shows a higher domain size than the TEOS-prepared V-MCM-41 catalysts. Furthermore, as expected, the dehydrated catalysts (in both cases) show an increase in the edge energy values, showing the possible transformation of the square pyramidal/octahedral coordination to its tetrahedral coordination upon expulsion of the coordinated water molecules (Table 2). Thus the increase in edge energy values upon dehydration shows a decreased electron density on the vanadium atom, which may arise from the loss of electron-donating H_2O species.

The EPR spectra of as-synthesized vanadium-containing mesoporous materials, recorded at room temperature, are given in Fig. 9A. The commonly used vanadium source for the synthesis of vanadium-containing mesoporous materials is vanadyl sulfate (V^{4+}, d^1), and in as-synthesized forms the material usually exhibits the characteristic eight-line hyperfine splitting (hfs) patterns due to the interaction of the unpaired electron with the nuclear spin of the ^{51}V nuclei ($I = 7/2$, natural abundance = 99.8%) [25]. However, it is

Table 2
Relative proportion of UV–vis spectra and the corresponding absorption edge energy values of vanadium silicates and vanadium model compounds

Catalyst	% of 240–270 nm site	Absorption edge energy (eV)	Domain size[a]	Local symmetry
VMT-55 (H)	77.77	3.67	–	–
VMT-55 (D)	> 95	4.11	–	–
VMS-55 (H)	70.92	3.31	–	–
VMS-55 (D)	91.23	3.60		–
Na_3VO_4	–	3.21	1.729	Tetrahedral
NH_4VO_3	–	3.23	1.735	Distorted tetrahedral
V_2O_5	–	2.30	1.978	Square pyramidal

[a] From Ref. [24].

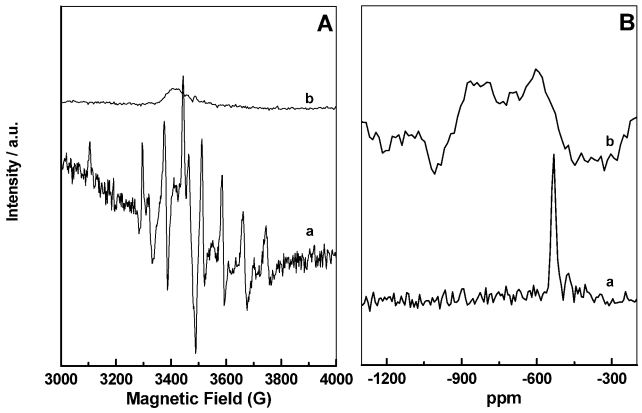

Fig. 9. EPR (A) and ^{51}V MAS NMR (B) spectra of V-MCM-41 catalysts, where (a) stands for VMS (Si/V = 55) and (b) stands for VMT (Si/V = 55) catalysts.

surprising to note that only the V-MCM-41 catalyst prepared from fumed silica had shown the typical hyperfine splitting pattern, whereas the material prepared from TEOS as the silica source shows the absence of hyperfine splitting patterns. The well-resolved hyperfine splitting patterns obtained for the VMS catalysts indicate that the $(VO)^{2+}$ ions are well dispersed inside the pore channels of the MCM materials, and the observed g values ($g_\parallel = 1.945$, $g_\perp = 1.997$) and the hyperfine coupling constants ($A_\parallel = 185$ G and $A_\perp = 68$ G) are in good agreement with the values for $(VO)^{2+}$ ions with a distorted pseudo-octahedral coordination [7]. Even though a proper comparison to distinguish the spectral patterns of VMS and VMT catalyst is difficult, Sayari et al. [4a] attributed the absence of EPR signals in vanadium-containing mesoporous materials to the presence of V^{4+} ions in highly symmetrical lattice positions and to the electronic degeneracy and associated very short relaxation times. Selvam et al. [26] also noted such results for V-MCM-41 materials and had assigned this surprising behavior to the aerial oxidation of V^{4+} to V^{5+} during high pH/hydrothermal synthesis conditions. Since the present synthesis procedures differ only with respect to the silica source, the former assignment is more likely, and thus the present study shows that such anomalous results may also arise from the nature of silica sources, which may have a role in the transformation of V^{4+} to V^{5+} and/or in the stabilization of V^{4+} species. Hence it is assumed that during the drying process the V^{4+} species prevailing inside the pores of the VMT catalyst is more likely to change its oxidation state to the EPR silent V^{5+}, and the better stability/capping of the V^{4+} species in the VMS matrix may help it to retain the tetravalent state.

In order to ascertain whether the absence of hfs patterns for VMT catalyst arise from any agglomerated V_2O_5 species, ^{51}V MAS NMR experiments were also carried out; the results are depicted in Fig. 9B. Since vanadium is 99.8% abundant and has a large magnetic moment and short spin relaxation times, judicial experimental procedures can provide information on the local coordination of vanadium atoms in the silica framework. Eckert and Wachs [27] showed nicely how the mass spectra vary over different field strengths and showed in detail the peak assignment values of supported vanadium catalysts and vanadium model compounds. Hence for the interpretation of various bands, their findings are followed, and thus the signals around −500 to −540 ppm, are assigned to the tetrahedrally coordinated vanadium sites. Since no signals are observed in the −300 ppm region, the formation of octahedrally coordinated V_2O_5 is discarded and thus suggests that most of the added vanadium is incorporated into the silica framework as tetrahedral coordination with the oxygen ligands. However, as in the EPR results, one can notice a sharp difference in spectra between the V-MCM-41 catalysts, that the VMS catalyst shows a sharp peak at ∼530 ppm, and the sample prepared from a TEOS silica source shows a less intense and broad peak with two maxima after −500 ppm. Since the differences arise from the interference between signals, we assume that vanadium exists not in a perfect tetrahedral position in VMT catalyst, but largely as disordered tetrahedral sites, and/or that the presence of different tetrahedral vanadium species on the VMT catalysts may be responsible for the multiple peak positions after −500 ppm, consistent with the earlier results [24].

In the characterization of metal-containing solid materials, Raman spectroscopy has been extensively used for the determination of isolated/clubbed metal sites, and it is generally accepted that the results obtained from this measurement are conclusive. Hence for a better confirmation of the nature of vanadium sites residing on V-MCM-41 materials, synthesized from different silica sources, Raman analysis is also performed. Fig. 10 depicts the Raman spectra of VMT and VMS samples, and for comparison, the spectrum of pure V_2O_5 is also given. The Raman bands observed at 480, 620, 810, and 972 cm^{-1} arise from the threefold and fourfold siloxane rings, whereas the latter two bands are assigned to the siloxane bridges and the silanol groups, which may arise from the inorganic backbone of the amorphous MCM-41 silica surface [7,28]. It is worth noting that the VMS sample shows a strong band at 1030 cm^{-1}, which is characteristic of isolated tetrahedrally coordinated terminal $(SiO)_3V{=}O$ groups, whereas such bands are not so prominent for the VMT catalyst. However, both samples produce bands at

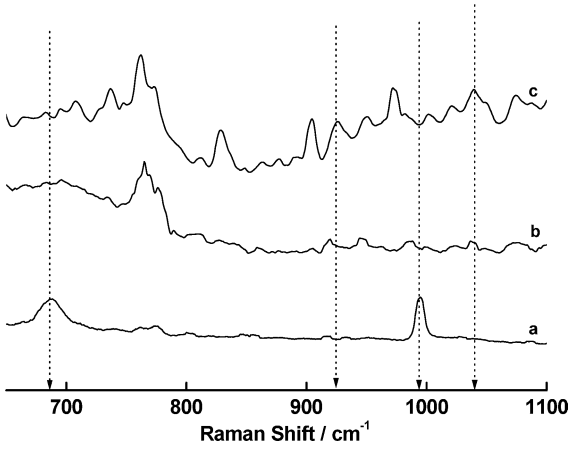

Fig. 10. Raman spectra of calcined vanadium containing catalysts, (a) V_2O_5, (b) VMT (Si/V = 55), (c) VMS (Si/V = 55).

1070 and 920 cm^{-1} and are attributed to the perturbed silica surfaces, which may arise because of the interference of neighboring vanadium atoms or because of Si–O–V moieties [29]. According to Can Li [30], high-frequency bands correspond to shorter V–O bonds, and hence the bands greater than 1000 cm^{-1} in the present case may correspond to the V–O species, which may arise from the isolated terminal metal sites, as mentioned earlier. Furthermore, in agreement with the UV–vis and ^{51}V NMR results, the Raman spectra did not show any band characteristic of crystalline V_2O_5 (usually observed around 995, 703, 530 cm^{-1}) and hence we conclude from all characterizations techniques that regardless of the silica source, vanadium exists in the form of isolated tetrahedral sites in V-MCM-41 catalysts, but in a more disordered tetrahedral environment in the case of VMT catalysts.

3.3. Catalytic results

Since the above characterization results showed that vanadium exists in the tetrahedral environment in both catalysts with slight differences, it may be highly active in various (ep)oxidation reactions with organic/inorganic peroxides as the oxidizing agent. Hence the present catalysts are applied in the liquid-phase epoxidation reaction of the cyclic olefin, cyclooctene, with different oxidizing agents, such as aqueous H_2O_2 (30%) and TBHP (70%). Since the physical properties of the two oxidizing agents are different, it may provide a qualitative idea of the existence of the vanadia species residing in the framework of the mesoporous sites and of its stability.

However, before evaluating the catalytic activity, we must to reconsider the processes usually occurring in liquid-phase epoxidation reactions with sacrificial oxidants like peroxides as oxygen donors. Usually H_2O_2 gets anchored on the active catalytic site, which may further react with the alkene to form the desired epoxide (route i); a parallel alternative reaction is the decomposition of peroxides to water (route ii). The drawback of route ii is the irreversible hydrolysis of the active metal center, which usually leads to decreased

Table 3
Epoxidation of cyclooctene over vanadium-containing catalysts synthesized using different silica sources[a]

Catalyst	Cyclooctene conversion[b] (mol%)	H_2O_2 conversion (%)	TOF[c] (h^{-1}) ($\times 10^2$)	Epoxide selectivity (mol%)
VMS (25)	28.1 (26.0)	78 (85)	10.4	97
Sil-VMS (25)	24.7 (25.2)	43 (80)	8.80	100
VMS (55)	50.3 (17.8)	53 (66)	39.0	> 99
VMS (83)	33.6 (10.3)	n.e.[d]	6.7	100
SMS	2.4	n.e.	–	100
VMT (25)	33.0 (22.8)	53 (80)	17.0	> 99
Sil-VMT (25)	24.0 (20.2)	42 (77)	11.0	100
VMT (55)	23.3 (14.8)	46 (70)	15.7	100
VMT (83)	10.6 (11.5)	n.e.	13.5	100
SMT	5.0	n.e.	–	100
No catalyst	1.6	n.e.	–	100

[a] Reaction conditions: $T = 343$ K, cyclooctene: oxidant = 4.0 mol/mol; catalyst weight = 10% of cyclooctene, solvent, CH_3CN = 5 ml, reaction time = 12 h. Values in parentheses show the results over TBHP oxidant.
[b] (Cyclooctene conversion/theoretically possible conversion) ×100.
[c] Turnover frequency (TOF) = moles of substrate converted/mole of vanadium per h.
[d] n.e. = not evaluated.

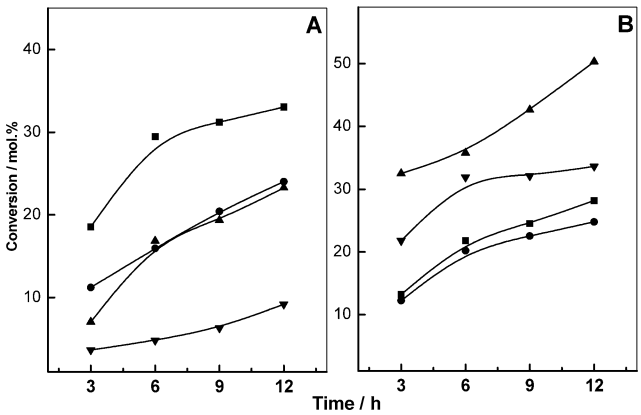

Fig. 11. Influence of reaction time in the conversion of cyclooctene over, (A) VMT catalysts and (B) VMS catalysts, where (■) Si/V = 25, (●) silylated Si/V = 25, (▲) Si/V = 55, (▼) Si/V = 80.

activity during recycling and the leaching of active metal sites. Hence to maintain the preferential formation of epoxide (route i) and to limit its drawbacks, due to the more aqueous nature, the oxidant concentration is kept as low as possible, thereby increasing the alkene reaction. Table 3 lists the conversion data for VMS and VMT catalysts of different vanadium loadings; under both the oxidizing atmospheres and in line with the characterization results, the fumed silica vanadium catalyst shows a better performance than the VMT catalysts. Thus the improved catalytic results for VMS catalysts compared with VMT catalysts may relate to the greater percentage of extraframework metal species on VMS catalysts compared with the TEOS-synthesized vanadium catalysts (Fig. 11). In addition, blank experiments carried out, without any catalyst or with vanadium-free silica show far fewer conversions, and hence the enhanced conversion

rate observed over vanadium-containing catalysts confirms the role of vanadium ions in the present reaction (Table 3). Another interesting result of the experiments is the increased catalytic activity of the VMS (55) catalyst compared with the VMS catalyst with the higher vanadium content (25). Earlier literature reports assigned such behavior to the formation of M–O–M bonds and/or to the loss of structural integrity of the mesoporous material at higher metal loadings [31,32]. However, in the present case, V-MCM-41 (25) had shown good-quality XRD patterns and hence the latter assumption can be avoided, and thus the decreased conversion rates may account for the slight oligomerization of vanadia species at higher metal loadings. Generally, octahedrally coordinated metal species, like V_2O_5, are less active in epoxidation reactions because of the lack of free coordination sites, and thus the low conversion rates for VMS (25) catalyst prove that the material may contain dimeric/oligomeric vanadia species, supported by its higher H_2O_2 decomposition rates. However, for the TEOS-synthesized V-MCM-41 catalysts the conversions increases monotonically with the vanadium content.

It is generally assumed that solvents have a tremendous influence on the catalytic activity and stability of various metal-containing mesoporous silicates, and the properties are largely attributed to the difference in the chelating abilities of the polar group of the solvent molecule with the metal sites. Apart from this, the role of solvents in oxidation reactions is too complicated to diagnose, since it varies with various factors, such as polarity, solubility of the reactants and formed products, diffusion limitations, etc. [33]. Even though a solvent-free atmosphere is appreciated under the present environmental regulations, negligible activity of the catalysts (<2%), under solvent-free conditions, led to the use of diluents for enhanced conversion rates. Among the solvents used, acetonitrile shows enhanced conversion rates, and the catalytic activity follows the order $CH_3CN > (CH_3)_2CO > CH_3OH$, regardless of the catalyst sample. The enhanced activity of the polar aprotic solvent may arise from a decreased phase separation between the aromatic alkene portion and the aqueous oxidant part, which in turn may allow easy transport of the active oxygen species for the epoxidation process [15]. Usually usage of more protic solvents increases the acidity of the catalyst surface and thereby increases the cleavage of the formed epoxide to its corresponding diol moieties. However, in the present epoxidation reaction of cyclooctene the large stability of the formed epoxide (epoxy cyclooctene) may be the reason for the increased selectivities (>98%), even after longer times and in the presence of catalysts with higher vanadium content.

It is well known that silylation of the catalyst surface enhances the catalytic activity of M-MCM-41-related materials as it changes the physical properties of the material from a more hydrophilic nature to hydrophobic [34]. Since the reactants applied under the present reaction or any (ep)oxidation reactions are of different polarities, a more hydrophobic catalyst can suitably adsorb the olefins more than aqueous oxidant and hence can produce epoxides in higher yields.

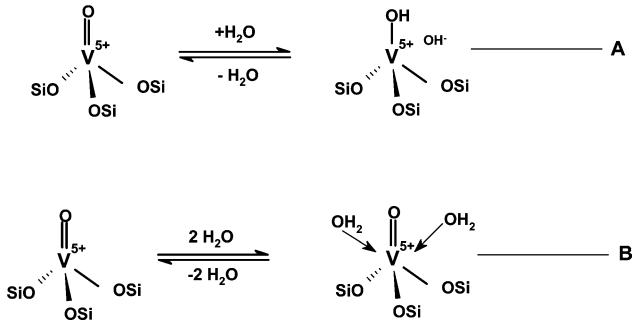

Scheme 1. Possible representation of vanadium sites in (A) VMT catalysts and (B) VMS catalysts.

Furthermore, the hydrophobic environment on the catalyst surface can diffuse the formed epoxide (which is polar) easily, and hence the subsequent cleavage of the oxirane ring can be greatly reduced. Thus, considering the case of improved hydrophobicity attained by the silylation procedures, it is likely that the conversion must increase in the more hydrophobically favorable environments. However, the concept "like adsorbs like" does not hold good for the silylated VMS or VMT catalyst (see Table 3), where the modified systems show a decreased conversion rate, which may be due to the blocking of some of the active sites inside the pore channels by the organic groups or to the loss of a slight amount of vanadium species (from extraframework) during modifications.

3.4. Structure/activity/stability correlations

Structural characterization of the developed catalysts shows that the material prepared from a fumed silica source displays better thermal and hydrothermal stability than the TEOS-synthesized vanadium catalysts, and spectroscopic evidence shows that vanadium exists in different tetrahedral environments over different silica sources. From UV–vis and edge energy measurements it can be seen that the TEOS-synthesized catalyst shows a greater percentage of framework-incorporated tetrahedral sites than the fumed silica catalyst, but the broadening of the ^{51}V NMR spectra reveals that the symmetry of vanadium species is not perfectly tetrahedral; they display more distorted states and the water of coordination is less pronounced. In contrast, the sharp and distinct ^{51}V NMR/Raman band in the VMS catalyst and the greater percentage of extraframework metal species on the VMS catalyst (rapid color change during hydration process) essentially show that the material consists of well-exposed $(SiO)_3V{=}O$ species probably located near the pore mouth, which allows an easy change in the coordination state of vanadium species with the hydration and rehydration processes. Hence considering the above spectral results and the suggestions put forward by Wei et al., we propose a possible representation of the vanadium sites on the two silica matrixes, as in Scheme 1 [24].

In order to determine whether the activity of the V-MCM-41 materials arises from stable mesoporous materials, we

also conducted a series of leaching studies, since they can provide some correlations with the mesostructure and activity. Since leaching of active metal species is a common phenomenon observed in mesoporous metallosilicates due to the destruction of the delicate solid pore wall surface under reaction conditions, stability/heterogenity studies are of primary importance for their further applicability. Since small amounts of leached metal species can have a significant effect on the entire catalytic activity, a rigorous proof of the heterogeneity of the catalyst is necessary and is usually promoted by the coordination ability of solvents on active metal sites and the use of aqueous oxidants (more aqueous oxidants are more prone to leaching, etc.). Hence in the present study we performed two leaching studies: (i) The catalyst applied under the reaction conditions was removed after a definite time interval, and the filtrate was monitored for further reaction rates. (ii) The catalyst was stirred (2 h) under the reaction conditions in the presence of solvent and to the catalyst removed "hot filtrate," substrate and oxidant were added to probe the conversion rates. Indeed, the former way of analysis is the crucial step, and out of curiosity we performed the first-step leaching study under hot and cold conditions. Sheldon et al. [35] showed for chromium-containing porous silicates that cold filtration steps show lower conversion rates than hot filtration steps because of the readsorption of dissolved metal ions from solution to the catalyst surface on cooling. However, the present studies on V-MCM-41 materials indicate that the leaching of vanadium species from MCM-41 matrix occurred under both conditions over both catalyst systems (Fig. 12). Furthermore, a combination of the above two stability tests explicitly shows that aqueous H_2O_2 is the actual culprit in promoting the leaching of active metal sites in case of V-MCM-41 catalyst systems, from a consideration of the amount of structural collapse, from PXRD measurements. Hence we tentatively attribute the leaching of vanadium in VMS catalysts to the extraframework metal sites, whereas for the VMT catalyst, the structural degradation of the meso framework may be the reason for leaching, from a consideration of the large attenuation in the XRD patterns for H_2O_2-treated VMT catalysts. These assumptions parallel the scheme proposed, and hence for a better design of V-MCM-41 catalysts, in the presence of H_2O_2 oxidants, a compromise between the above two is essential. Interestingly, although the conversion rates are lower with the TBHP oxidant, the crucial point is that the spent VMT catalyst retains ∼70% of the structural ordering in place of completely amorphous material obtained after H_2O_2 treatments. Thus use of TBHP as an oxidant implies a possible reusability of the catalyst materials, since regular structural patterns of mesoporous materials may always tend to make the metal sites more accessible for the diffused reactant species [18]. Hence the increased stability and the structural perfection observed for VMS catalysts (after H_2O_2/TBHP treatments) show that the inorganic backbone arising from the fumed silica source is far better than the TEOS-synthesized catalysts. Furthermore, since the vanadium species in V-MCM-41 materials are never bound to four silicate species after calcination, for a profound applicability and reusability, use of less aqueous oxidants like TBHP and catalysts with lower vanadium contents and a judicial choice of the silica source (fumed silica instead of TEOS) is proposed.

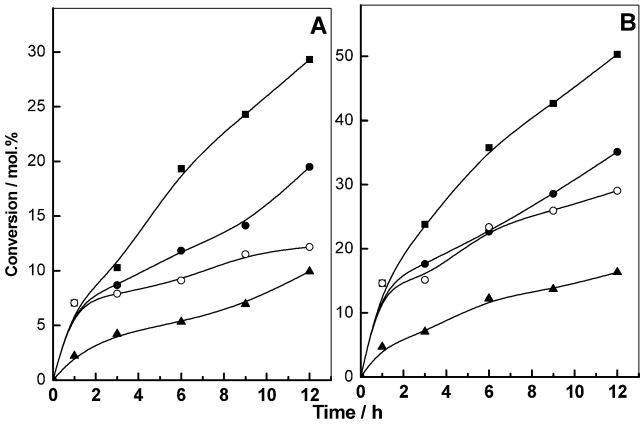

Fig. 12. Various leaching studies performed over V-MCM-41 catalysts, (A) VMS and (B) VMT catalysts: where, (■) stands for fresh cycle, (●) reaction temperature filtration of catalyst, after 1 h run (hot filtration), (○) room temperature filtration of catalyst, after 1 h run (cold filtration), (▲) catalyst was stirred in solvent for 2 h, and the filtrate obtained was applied to the reaction conditions with substrate and oxidant.

4. Conclusions

Vanadium-substituted mesoporous MCM-41 materials were synthesized hydrothermally with vanadyl sulfate as the metal precursor and fumed silica and tetraethyl orthosilicate as the silica sources. Characterization techniques revealed that, regardless of the silica source, the textural properties of the mesoporous support increase monotonically with vanadium loading, and detailed spectroscopic characterization techniques revealed the presence of a more isolated tetrahedral vanadium site on the VMS catalyst than on the VMT catalyst. Thermal and hydrothermal stability of V-MCM-41 materials shows that the materials prepared from a fumed silica source are more resistant to severe treatment conditions and are correlated with the increased silica condensation of the V-MCM-41 materials. Recycling studies and the characterization of spent catalysts indicate that the materials synthesized from a fumed silica source are structurally more stable than the TEOS-synthesized material and are suggested to arise from the higher degree of silicate condensation, which in turn will increase the wall thickness and thereby its structural integrity.

Acknowledgments

We thank Drs. D. Srinivas, N.E. Jacob, N.R. Shiju, and Ms. G. Kavitha for characterization results and useful discussions. S.S. thanks CSIR, India, for a senior research

fellowship and acknowledges the CSIR task force project (scheme under "Catalysts and Catalysis"/P23-CMM 0005-B) for financial assistance.

References

[1] C.T. Kresge, M.E. Leonowicz, W.J. Roth, J.C. Vartuli, J.S. Beck, Nature 359 (1992) 710.
[2] (a) D. Brunel, Micropor. Mesopor. Mater. 27 (1999) 329;
(b) A. Stein, B.J. Melde, R.C. Schroden, Adv. Mater. 12 (2000) 1403.
[3] J.Y. Wing, C.P. Mehnert, M.S. Wong, Angew. Chem. Int. Ed. Engl. 38 (1999) 56.
[4] A. Sayari, Chem. Mater. 8 (1996) 1840, and references therein;
(b) A. Corma, Chem. Rev. 97 (1997) 2373.
[5] M. Morey, A. Davidson, H. Eckert, G.D. Stucky, Chem. Mater. 8 (1996) 486.
[6] K.M. Reddy, I. Moudrakovski, A. Sayari, J. Chem. Soc., Chem. Commun. (1994) 1059.
[7] M. Mathieu, P. Vander Voort, B.M. Weckhuysen, R.R. Rao, G. Catana, R.A. Schoonheydt, E.F. Vansant, J. Phys. Chem. B 105 (2001) 3393.
[8] J.S. Reddy, P. Liu, A. Sayari, Appl. Catal. A: Gen. 148 (1996) 721.
[9] M. Chatterjee, T. Iwasaki, H. Hayashi, Y. Onodera, T. Ebina, T. Nagase, Chem. Mater. 11 (1999) 1368.
[10] S. Gontier, A. Tuel, Micropor. Mater. 5 (1995) 161.
[11] Z. Luan, J. Xu, H. He, J. Klinowski, L. Kevan, J. Phys. Chem. 100 (1996) 19595.
[12] Y. Deng, C. Lettmann, W.F. Maier, Appl. Catal. A: Gen. 214 (2001) 31.
[13] B.J. Whittington, J.R. Anderson, J. Phys. Chem. 97 (1993) 1032.
[14] (a) L. Chen, T. Horiuchi, T. Mori, K. Maeda, J. Phys. Chem. B 103 (1999) 1216;
(b) K. Cassiers, T. Linssen, M. Mathieu, M. Benjelloun, K. Schrijnemakers, P. Vander Voort, P. Cool, E.F. Vansant, Chem. Mater. 14 (2002) 2317.
[15] S. Shylesh, A.P. Singh, J. Catal. 228 (2004) 333.
[16] Q. Huo, D.I. Margolese, G.D. Stucky, Chem. Mater. 8 (1996) 1147.
[17] S. Lim, G.L. Haller, J. Phys. Chem. B 106 (2002) 8437.
[18] V. Parvulescu, C. Anastasescu, B.L. Su, J. Mol. Catal. A: Chem. 3919 (2003) 1.
[19] (a) J.R. Sohn, Zeolites 6 (1986) 225;
(b) G.N. Vayssilov, Catal. Rev. (1997) 209.
[20] B.M. Reddy, I. Ganesh, B. Chowdary, Catal. Today 49 (1999) 115.
[21] W. Zhang, M. Froba, J. Wang, P.T. Tanev, J. Wong, T.J. Pinnavaia, J. Am. Chem. Soc. 118 (1996) 9164.
[22] D.G. Barton, M. Shtein, R.D. Wilson, S.L. Soled, E. Iglesia, J. Phys. Chem. B 104 (2000) 1516.
[23] R.S. Weber, J. Catal. 151 (1995) 470.
[24] D. Wei, H. Wang, X. Feng, W.T. Chueh, P. Ravikovitch, M. Lyubovsky, C. Li, T. Takeguchi, G.L. Haller, J. Phys. Chem. B 103 (1999) 2113, and references therein.
[25] (a) S.K. Mohapatra, P. Selvam, Catal. Lett. 93 (2004) 47;
(b) P. Selvam, S.E. Dapurkar, J. Catal. 229 (2005) 64.
[26] P. Selvam, S.E. Dapurkar, Appl. Catal. A: Gen. 276 (2004) 257.
[27] H. Eckert, I.E. Wachs, J. Phys. Chem. 93 (1989) 6796.
[28] K.J. Chao, C.N. Wu, H. Chang, L.J. Lee, S. Hu, J. Phys. Chem. B 101 (1997) 6341.
[29] X. Gao, S.R. Bare, B.M. Weckhuysen, I.E. Wachs, J. Phys. Chem. B 102 (1998) 10842.
[30] G. Xiong, C. Li, H. Li, Q. Xin, Z. Feng, Chem. Commun. (2000) 677.
[31] N.N. Trukhan, V.N. Romannikov, E.A. Paukshtis, A.N. Shmakov, O.A. Kholdeeva, J. Catal. 202 (2001) 110.
[32] O.A. Kholdeeva, A. Derevyankin, A.N. Shmakov, N.N. Trukhan, E.A. Paukshtis, A. Tuel, V.N. Romannikov, J. Mol. Catal. A: Chem. 158 (2000) 417.
[33] A. Corma, P. Esteve, A. Martinez, J. Catal. 161 (1996) 11.
[34] P. Wu, T. Tatsumi, T. Komatsu, T. Yashima, Chem. Mater. 14 (2002) 1657.
[35] H.E.B. Lempers, R.A. Sheldon, J. Catal. 175 (1998) 62.